

doi:10.15199/48.2021.12.28

Optimizing the control of a brushless DC motor

Abstract. The paper proposes a strategy for controlling a brushless DC motor excited by permanent magnets. The results of investigations are presented. The investigations were carried out to determine the impact of the proposed control optimization on the dynamics of the drive system during starting the motor and during the steady operation of the system with the motor loaded. The cases of an open-loop system with the use of a voltage reference adjuster and a cascade structure with the use of closed loops for controlling the electromagnetic torque and angular velocity of the motor were considered.

Streszczenie. W pracy zaproponowano strategię sterowania bezszczotkowym silnikiem prądu stałego wzbudzonym magnesami trwałymi. Zaprezentowano wyniki badań, przeprowadzonych w celu ustalenia wpływu proponowanej optymalizacji sterowania na dynamikę układu napędowego podczas rozruchu silnika oraz w czasie ustalonej pracy układu z obciążonym silnikiem. Rozważono przypadki układu pracującego z otwartą pętlą, z wykorzystaniem zadajnika napięcia oraz struktury kaskadowej z zastosowaniem zamkniętych obwodów regulacji momentu elektromagnetycznego i prędkości kątownej silnika (**Optymalizacja sterowania bezszczotkowym silnikiem prądu stałego**).

Keywords: BLDC motor, back EMF, control strategies and optimization, measurement of angular position.

Słowa kluczowe: silnik BLDC, napięcia indukowane, strategie i optymalizacja sterowania, pomiar położenia kątownego.

Introduction

Electric motors excited by permanent magnets, which include a brushless DC motor (BLDC motor) [1–6] and a permanent magnet synchronous motor (PMSM) [7–9], are used in many branches of the economy, including the tool industry, automotive, medical, industrial automation, etc. There are two types of brushless motors excited by permanent magnets: motors with trapezoidal back Electromotive Force (EMF) waveform (applies mainly to BLDC motors) and motors with sinusoidal back EMF waveform (applies mainly to PMSM). This division results from different ways of connecting the turns (coils) forming the stator winding and different ways of forming the magnetic field distribution in the motor air-gap by appropriate magnetization of permanent magnets or shaping the rotor pole pieces. In the case of a motor with a sinusoidal waveform of back EMF, both phase voltages and phase currents change in a sinusoidal manner, and the electromagnetic moment has a smooth waveform, in contrast to the distorted waveforms of back EMF and phase currents as well as the rippled electromagnetic torque of the motor with a trapezoidal back EMF waveform, which are the cause of the additional vibration and noise.

The brushless DC motor is a combination of a permanent magnet synchronous motor and an electronic commutator (inverter). It is possible to activate semiconductor switches (transistors) of the inverter supplying the synchronous motor from an independent voltage-controlled pulse generator or from an angular position transducer coupled with the motor shaft. In the latter case, the effect of switching the stator phase windings in certain rotor positions is analogous to the operation of a mechanical commutator in a brushed DC motor. The properties of the synchronous motor controlled in this way are then similar to those of a separately excited DC motor.

In order to determine the angular position of a BLDC motor rotor, Hall sensors embedded in the stator are most often used, which together with permanent magnets mounted on the rotor form a magnetic encoder. Instead of a magnetic encoder, optical encoders or rotary electrical transformers, two-phase (resolver) or three-phase (synchro), can be used to measure the angular position of the rotor [6]. Contrary to the most popular optical encoders, rotary electrical transformers are resistant to vibration, shock, dust and moisture, and to long-term operation at high temperatures. Their disadvantage is the lower

accuracy of the measurement. The rotor of the rotary electrical transformer is excited with alternating current with a carrier frequency at least ten times higher than the frequency corresponding to the maximum speed of the motor. The magnetic field produced by the rotor current induces back EMFs in the stator phase windings.

In BLDC motor control, the Pulse Width Modulation (PWM) method is frequently used to limit the starting current as well as to control the speed and torque of the motor.

Proposed strategies for controlling brushless DC motors

The improvement of the parameters of control systems is a common pursuit of designers and users of these systems. In [6], a strategy for controlling a permanent magnet motor with a sinusoidal back EMF waveform having the properties of a DC motor as a result of using a synchro coupled with the motor shaft to drive the inverter, was proposed. This control strategy is explained in Fig. 1.

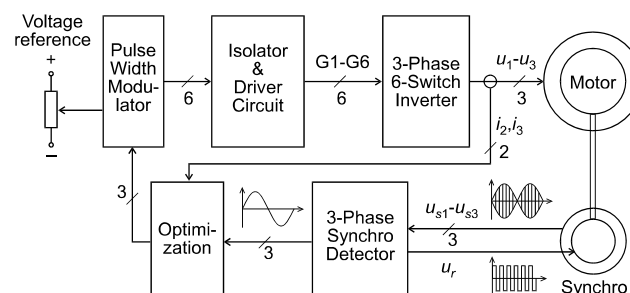


Fig. 1. Block diagram of the structure corresponding to the proposed control strategy for the BLDC motor with a sinusoidal back EMF waveform [6]

In the proposed control strategy, the optimization described by the dependencies (1), (2) and (3) was applied:

$$(1) \quad \sin \delta = \frac{Li_q}{\sqrt{L^2 i_q^2 + \psi_M^2}}, \quad \cos \delta = \frac{\psi_M}{\sqrt{L^2 i_q^2 + \psi_M^2}}$$

$$(2) \begin{bmatrix} a_1 \\ a_2 \\ a_3 \end{bmatrix} = \begin{bmatrix} \cos \delta \\ \cos(\delta - 120^\circ) \\ \cos(\delta + 120^\circ) \end{bmatrix} = \frac{1}{2} \begin{bmatrix} 2 \cos \delta \\ -\cos \delta + \sqrt{3} \sin \delta \\ -\cos \delta - \sqrt{3} \sin \delta \end{bmatrix}$$

$$(3) \begin{bmatrix} u_{\delta 1} \\ u_{\delta 2} \\ u_{\delta 3} \end{bmatrix} = \frac{2}{3} \begin{bmatrix} a_1 & a_3 & a_2 \\ a_2 & a_1 & a_3 \\ a_3 & a_2 & a_1 \end{bmatrix} \begin{bmatrix} u_{d1} \\ u_{d2} \\ u_{d3} \end{bmatrix}$$

where: $u_{d1,2,3}$ are voltages at the output of the 3-Phase Synchro Detector, $u_{\delta 1,2,3}$ are voltages at the output of the Optimization block.

Other quantities in dependencies (1) are the inductance of the motor winding, the flux linkage excited by permanent magnets and the quadrature component of the space vector of the motor current in the reference system related to the magnetic poles of the rotor and defining the magnitude of the electromagnetic moment.

Figure 2 shows the waveforms of the electromagnetic torque (τ_e), angular velocity (ω) and phase current (i) during the start-up of a 4 kW BLDC motor.

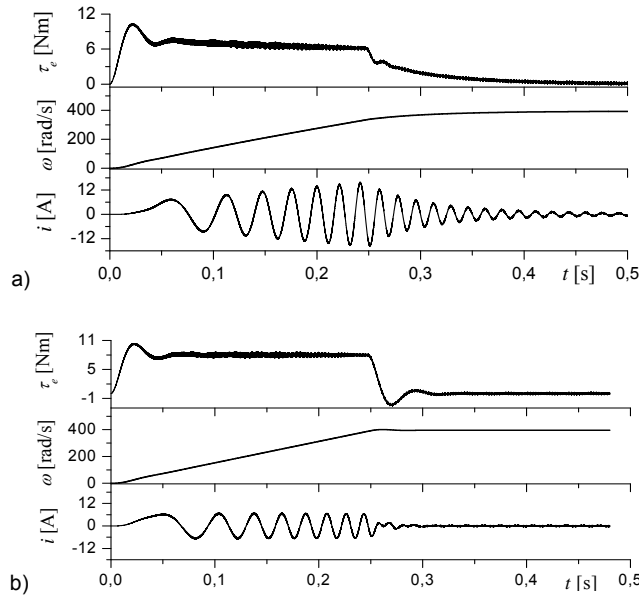


Fig.2. Waveforms of electromagnetic torque, angular velocity and phase current during the starting of a motor with a sinusoidal waveform of the back EMF, in the system shown in Fig. 1, with optimization turned off (a) and optimization turned on (b)

As a result of the optimization applied to the drive system with a permanent magnet motor with a sinusoidal back EMF waveform, powered from an inverter driven by a rotary electrical transformer coupled with the motor shaft, the dynamics of the system was improved, without the use of closed loops for controlling the armature current or electromagnetic torque and angular velocity, and their synthesis. This improvement is manifested by a reduction in the starting current amplitude, an even level of electromagnetic torque during start-up, and a shortened start-up time.

The use of the dependencies (1), (2) and (3) in the control system of a motor with a trapezoidal back EMF waveform (see Fig. 3) leads to its commutation with a phase advance (positive phase shift) by the angle δ depending on the load.

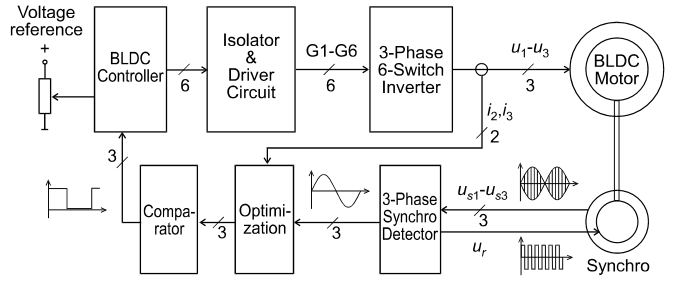


Fig.3. Block diagram of the structure corresponding to the proposed control strategy used for the motor with a trapezoidal back EMF waveform

Results of investigations

The investigations of the proposed structure for controlling the BLDC motor were performed with the use of the digital simulation method. The investigations were based on BLDC motor mathematical model formulated and tested by the authors [1]. The following equations formulate the matrix form of the BLDC motor mathematical model:

$$(4) \begin{bmatrix} u_a \\ u_b \\ u_c \end{bmatrix} = R \begin{bmatrix} i_a \\ i_b \\ i_c \end{bmatrix} + \frac{d}{dt} \begin{bmatrix} \psi_a \\ \psi_b \\ \psi_c \end{bmatrix} + \begin{bmatrix} e_a \\ e_b \\ e_c \end{bmatrix}$$

$$(5) \begin{bmatrix} \psi_a \\ \psi_b \\ \psi_c \end{bmatrix} = \begin{bmatrix} L & M & M \\ M & L & M \\ M & M & L \end{bmatrix} \begin{bmatrix} i_a \\ i_b \\ i_c \end{bmatrix}$$

where: $u_a, u_b, u_c, i_a, i_b, i_c, \psi_a, \psi_b, \psi_c$ are phase voltages, currents and flux linkages, e_a, e_b, e_c are back EMFs induced in the respective phase windings, $L = L_\sigma + L_\mu, M = -L_\mu/3, L_\mu$ is inductance of the main magnetic circuit (magnetization inductance), L_σ is leakage inductance. The following formula can be used to derive the phase currents from the matrix dependency (5):

$$(6) i_k = (L - M)^{-1} \left(\psi_k - M(L + 2M)^{-1} \sum_j \psi_j \right), \quad k, j = a, b, c$$

The currents derived above should be substituted into equation (4) in order to reduce the number of unknowns. Back EMFs can be defined as follows:

$$(7) \begin{bmatrix} e_a \\ e_b \\ e_c \end{bmatrix} = N_p \Psi_p \omega_m \begin{bmatrix} f_a(\theta_e) \\ f_b(\theta_e) \\ f_c(\theta_e) \end{bmatrix}$$

where Ψ_p is flux linkage excited by permanent magnets, ω_m is angular velocity of rotor, N_p is number of pole pairs. The following dependency can be used to approximate the functions f_a, f_b, f_c :

$$(8) \begin{bmatrix} f_a(\theta_e) \\ f_b(\theta_e) \\ f_c(\theta_e) \end{bmatrix} = k_f \begin{bmatrix} \sin(\theta_e) \\ \sin(\theta_e - 120^\circ) \\ \sin(\theta_e - 240^\circ) \end{bmatrix} \quad \begin{matrix} -1 \leq f_a(\theta_e) \leq +1 \\ -1 \leq f_b(\theta_e) \leq +1 \\ -1 \leq f_c(\theta_e) \leq +1 \end{matrix}$$

where: $k_f = 2$ for the approximation of the trapezoidal EMF with a wide trapezoid base (120 electrical degrees), $k_f = 1.2$ for the approximation of the trapezoidal EMF with a narrow trapezoid base (about 60 electrical degrees) and $k_f = 1$ for the approximation of the sinusoidal EMF.

The electromagnetic torque can be expressed as follows:

$$(9) \quad \tau_e = \omega_m^{-1} (e_a i_a + e_b i_b + e_c i_c)$$

Taking into account Equation 7:

$$(10) \quad \tau_e = N_p \Psi_P (f_a(\theta_e) i_a + f_b(\theta_e) i_b + f_c(\theta_e) i_c)$$

Figures 4 to 6 show the waveforms, respectively, of the phase current (i), electromagnetic torque (τ_e) and angular velocity of the rotor (ω) during the 4 kW BLDC motor start-up in the system shown in Fig. 3, with optimization turned off (a) and optimization turned on (b).

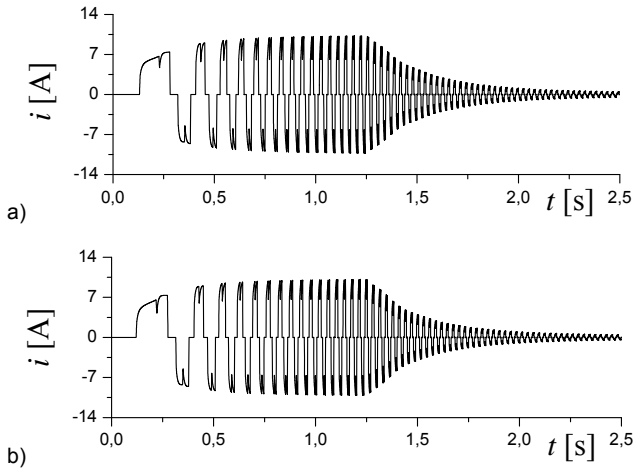


Fig.4. Phase current waveforms of the BLDC motor during the start-up in the system shown in Fig. 3, with optimization turned off (a) and optimization turned on (b)

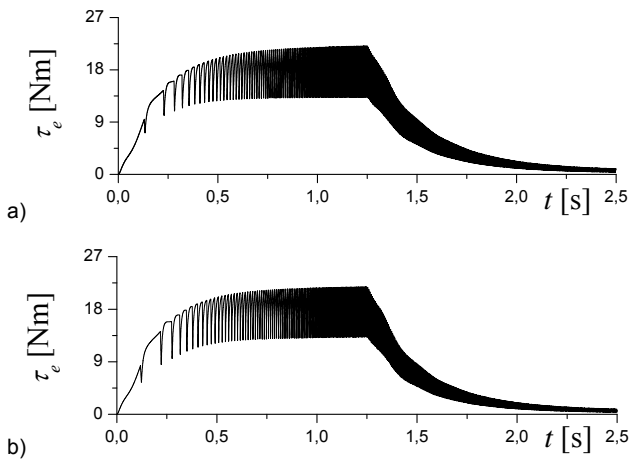


Fig.5. Waveforms of electromagnetic torque during BLDC motor start-up in the system shown in Fig. 3, with optimization turned off (a) and optimization turned on (b)

In the presented waveforms for BLDC the motor start-up, a slight reduction in the amplitude of the electromagnetic torque ripple and motor current ripple can be observed. On the other hand, no improvement in the dynamics of the system during the start-up, which would be manifested in a more even level of the electromagnetic torque during start-up and a shortened start-up time, was observed.

Figures 7 and 8 show the steady phase current and electromagnetic torque waveforms of the loaded BLDC motor in the system shown in Fig. 3, with optimization turned off (a) and optimization turned on (b).

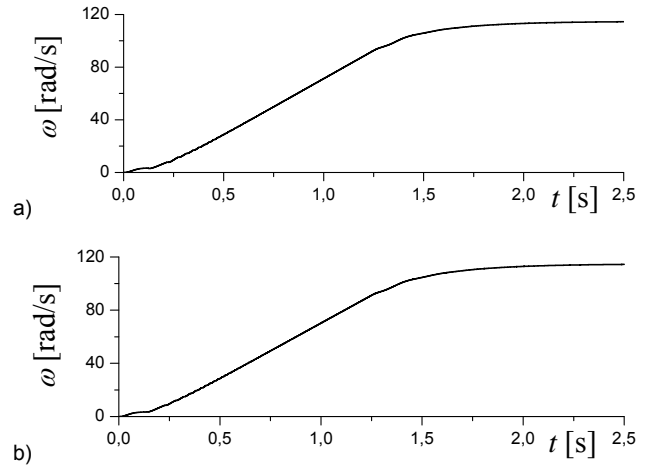


Fig.6. The angular velocity of the BLDC motor during the start-up in the system shown in Fig. 3, with optimization turned off (a) and optimization turned on (b)

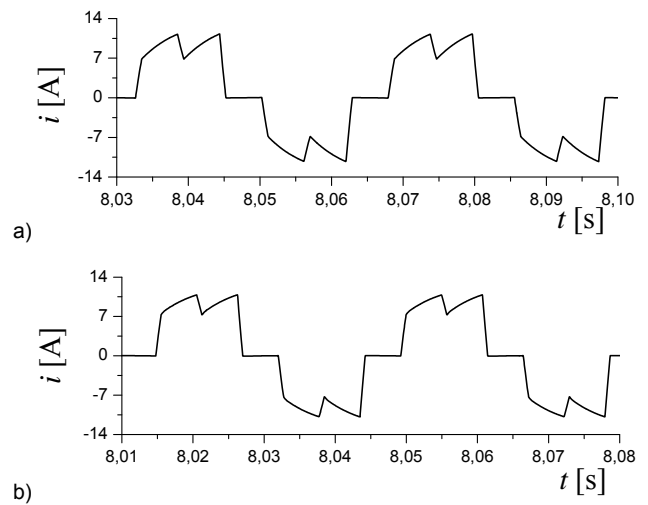


Fig.7. Waveforms of the phase current of a BLDC motor loaded with a rated torque in the system shown in Fig. 3, with optimization turned off (a) and optimization turned on (b)

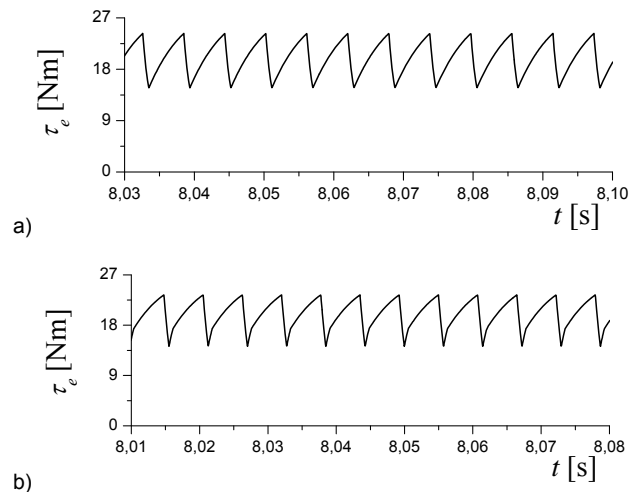


Fig.8. Waveforms of the electromagnetic torque of a BLDC motor loaded with rated torque in the system shown in Fig. 3, with optimization turned off (a) and optimization turned on (b)

The presented in Fig. 7 and Fig. 8 waveforms show the beneficial effect of the applied optimization on the parameters of the current and electromagnetic torque

waveforms, which is manifested in the reduction of the ripple amplitude of both quantities.

Figures 9 and 10 show the steady phase current and electromagnetic torque waveforms of a loaded BLDC motor in the angular velocity control system based on the structure from Fig. 3, in which, instead of the voltage reference adjuster, a cascade structure containing closed loops for controlling the electromagnetic torque and angular velocity are used, with the optimization turned-off (a) and optimization turned-on (b).

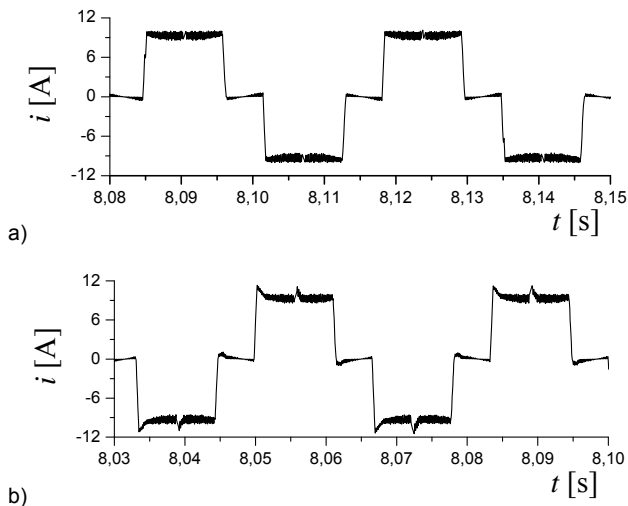


Fig.9. Phase current waveforms of a BLDC motor in the cascade angular velocity control system based on the structure from Fig.3, with optimization turned off (a) and optimization turned on (b)

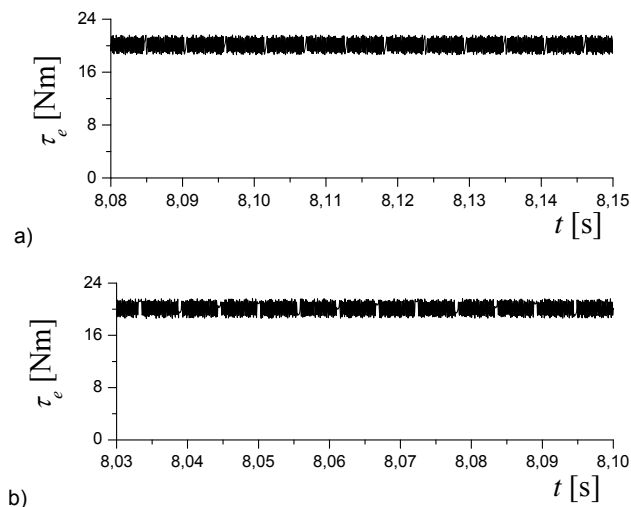


Fig.10. BLDC motor torque waveforms in the cascade angular velocity control system based on the structure from Fig. 3, with optimization turned off (a) and optimization turned on (b)

In the case of a cascade control structure containing closed loops for controlling the electromagnetic torque or armature current and the angular velocity of a BLDC motor with a trapezoidal back EMF waveform, the effect of the applied optimization is not favourable, as it results in the appearance of additional motor current distortions.

Conclusions

The paper proposes a strategy for controlling a brushless DC motor excited by permanent magnets with a trapezoidal back EMF waveform. This strategy was previously proposed and tested for a permanent magnet motor with a sinusoidal back EMF waveform, powered from an inverter driven by a rotary electrical transformer (synchro) coupled with the motor shaft, i.e. a motor with properties similar to those of a separately excited DC motor. The conducted research has shown a negligible influence of the proposed control optimization for BLDC motor with a trapezoidal back EMF waveform on the dynamics of the drive system, e.g. when starting the motor. On the other hand, one can observe a beneficial effect of the commutation of the motor with the positive phase shift, resulting from the optimization applied, on the parameters of the current and electromagnetic torque waveforms, manifested by the reduction of the amplitude of ripples of both quantities.

Authors: dr hab. inż. Andrzej Popena profesor uczelni, mgr inż. Marcjn Nowak, Politechnika Częstochowska, Katedra Elektroenergetyki, al. Armii Krajowej 17, 42-200 Częstochowa, E-mail: andrzej.popena@pcz.pl, marcjn.nowak@pcz.pl.

REFERENCES

- [1] Popena A., Modelling of BLDC motor energized by different converter systems, *Przegląd Elektrotechniczny*, 94 (2018), nr 1, 81-84
- [2] Yedamale P., *Brushless DC (BLDC) Motor Fundamentals*, Microchip Technology Inc., U.S.A., 2003
- [3] Rusek A., Chaban A., Lis M., A Mathematical Model of a Synchronous Drive with Protrude Poles, an Analysis Using Variational Methods, *Przegląd Elektrotechniczny*, 89 (2013), nr 4, 106-108
- [4] Lis M., Algorytm obliczenia wybranych parametrów różniczkowych silnika bezszczotkowego o wzbudzeniu od magnesów trwałych o sterowaniu trapezoidalnym (BLDC), *Przegląd Elektrotechniczny*, 88 (2012), nr 9a, 116-118
- [5] Nowak M., Analiza stanów dynamicznych układu napędowego zawierającego silnik BLDC oraz długi element sprężysty, *Przegląd Elektrotechniczny*, 89 (2013), nr 12, 302-305
- [6] Popena A., A control strategy of a BLDC motor, *Przegląd Elektrotechniczny*, 89 (2013), nr 12, 188-191
- [7] Shchur I., Rusek A., Mandzyuk M., Power Effective Work of PMSM in Electric Vehicles at the Account of Magnetic Saturation and Iron Losses, *Przegląd Elektrotechniczny*, 91 (2015), nr 1, 199-202
- [8] Olesiak K., Application of a Fuzzy Logic Controller for a Permanent Magnet Synchronous Machine Drive, *Przegląd Elektrotechniczny*, 92 (2016), nr 12, 113-116
- [9] Jakubiec B., Napęd pojazdu elektrycznego z wielofazowym silnikiem synchronicznym z magnesami trwałymi, *Przegląd Elektrotechniczny*, 91 (2015), nr 12, 125-128
- [10] Chaban A., Łukasik Z., Lis M., Szafraniec A., Mathematical Modeling of Transient Processes in Magnetic Suspension of Maglev Trains, *Energies*, 13 (2020), nr 24, 6642, 1-17
- [11] Lis M., Czaban A., Szafraniec A., Levoniuk V., Figura R., Mathematical modelling of transient electromagnetic processes in a power grid, *Przegląd Elektrotechniczny*, 95 (2019), nr 12, 160-163
- [12] Chaban A., Lis M., Szafraniec A., Jedynek R., Application of Genetic Algorithm Elements to Modelling of Rotation Processes in Motion Transmission Including a Long Shaft, *Energies*, 14 (2020), nr 1, 115, 1-17